Meteorological Modulation of the North Atlantic Spring Bloom.

Michael Follows and Stephanie Dutkiewicz

Department of Earth, Atmospheric and Planetary Sciences, Massachusetts Institute of Technology, 77 Massachusetts Avenue, Cambridge, MA 02139, USA.

Abstract

Using ocean time-series observations and remote chlorophyll estimates derived from SeaWiFS ocean color observations we examine and illustrate the relationships between changes in the intensity of the spring bloom and changes in weather patterns, mediated by upper ocean mixing. A simplified two-layer model provides the conceptual framework, predicting regional regimes of differing biological response to vertical mixing anomalies in the ocean surface boundary layer. The meteorological anomalies may be derived from re-analyzed meteorological data.

We examine two regimes of regional and interannual sensitivity to meteorological forcing, defined by the ratio of the spring critical layer depth and the winter mixed layer depth, h_c/h_m. Regions of large h_c/h_m (subtropics) are characterized by an enhanced bloom in response to enhanced mixing, both across the region and from year to year. The subtropics exhibit consistent, interannual changes which are coordinated over large regions, and local interannual changes are comparable in magnitude to the regional variations in each bloom. In the low h_c/h_m regime (subpolar), regional variations reflect retardation of the bloom by enhanced mixing. Local interannual changes in the subpolar region, however, are small relative to the regional variations and do not show a clear and consistent response to interannual variability in the local meteorological forcing. We infer that other factors, including changes in insolation, local mesoscale variability, and grazing exert a stronger influence on local interannual variability of the subpolar bloom.

We discuss the implications of these relationships for the implications of decadal climate changes on biological productivity.

1 Introduction.

We seek to understand the mechanistic connections between regional and interannual meteorological change, and variability in biological productivity.

Through the observation and understanding of such regional and interannual connections we may better understand how the climate system influences ocean bio-geochemistry. Here, more specifically, we identify mechanistic connections between local meteorological change (which may be associated with broader scale patterns of shifting climate regimes) and biological productivity during the spring bloom period.

Several studies have suggested that local, interannual and decadal variability of plankton in the North Atlantic are related to changes in regional climate and patterns of meteorological forcing. Aebischer et al.(1990), Fromentin and Planque (1998), Taylor and Stephens (1980) and Reid et al.(1998) have discussed the variability of the Continuous Plankton Recorder (CPR) data set for the Northern North-East Atlantic and North Sea. Correlations are found between plankton variability and indicators of local weather and climate shifts, such as the North Atlantic Oscillation and the position of the north wall of the Gulf Stream. These observations suggest that local variability in plankton may be in response to shifts in patterns of regional climate change.

Estimates of surface ocean chlorophyll from space, with excellent temporal and spatial resolution, provide an opportunity to reveal the underlying connections more clearly. The ongoing Sea-viewing Wide Field-of-view Sensor (SeaWiFS) mission already reveals significant interannual change which exhibits structure on many scales (Fig. 1). Here we seek to explain aspects of the regional and interannual changes in the SeaWiFS data set in terms of meteorological forcing and air-sea interactions, guided by a highly idealized model framework which connects the two through upper ocean mixing processes.

1.1 Upper Ocean Mixing and the North Atlantic Spring Bloom.

Menzel and Ryther (1961) observed that phytoplankton are nutrient limited in the Sargasso Sea, and the bloom generally occurs when the mixed layer is deepest, closely following the entrainment of of nutrients. In contrast, at mid- and high-latitudes, light limitation dominates and the bloom is initiated by the springtime restratification of the water column (Sverdrup, 1953). Sverdrup devised a depth scale, the "critical layer", in which the growth of phytoplankton exceeds mortality and respiration. He hypothesized that a bloom would occur when the mixed layer became shallower than this critical layer in the spring. Thus the bloom occurs progressively later in higher latitudes as insolation increases and the water column stratifies. This temporal shift of the bloom with latitude has been discussed (Cushing, 1959) and observed from space (Yoder et al., 1993; Kennelly et al., 2000).

Over large regions of the basin the bloom dynamics may be described by

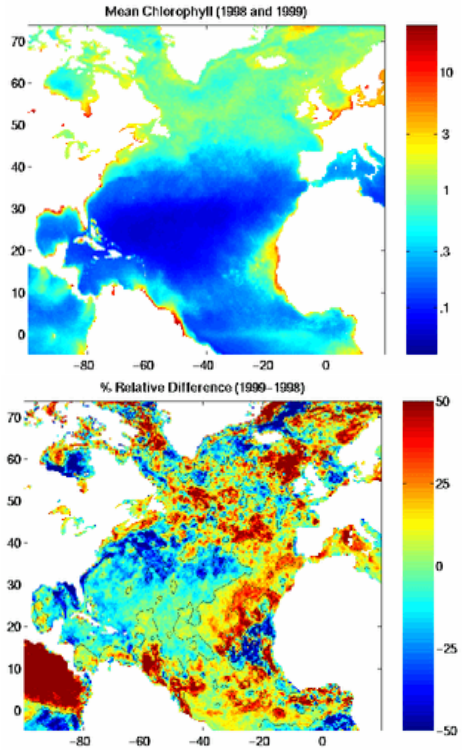

Fig. 1. Upper panel: Two year mean (1998 and 1999) surface chlorophyll concentration (mg/m^3) from SeaWiFS (Level 3, version 3) estimates. Lower panel: Relative difference (1999-1998) presented as a percentage of the mean. Contours are overlaid for -50%,-25%, 0%, 25% and 50% of the difference field.

the local vertical balance between the entrainment of nutrients (i.e. nitrate and phosphate) and the retention of phytoplankton within the euphotic layer. Both are strongly coupled to local vertical mixing in the upper ocean boundary layer. We note, however, that in some regions other influences such as nitrogen fixation (Michaels et al., 1994), lateral advection (Williams and Follows, 1998; Dutkiewicz et al., 2001) or mesoscale motions (McGillicuddy and Robinson, 1997) have a significant impact.

The springtime shoaling of the mixed layer is not typically a smooth transition, but is punctuated by mixing events stimulated by the passage of weather systems (Stramska et al., 1995). The frequency and intensity of these events varies from year to year with the shifting of storm tracks and modes of atmospheric circulation (Dickson et al., 1996). Enhanced storminess, and the subsequent increase in vertical mixing in the upper ocean, during spring could increase the amplitude of the bloom through enhanced nutrient supply, or retard it due to light limitation.

The effect of such changes in storminess and upper ocean mixing during the annual phytoplankton bloom was addressed in Dutkiewicz et al.(2001), hereafter DFMG, using a hierarchy of numerical models: A highly idealized, two-layer,

bio-physical description of the ocean's seasonal boundary layer, and a more complex, general circulation-ecosystem model. The idealized model of DFMG identifies the regimes in which enhanced mixing can either increase or decrease the bloom intensity, both from region to region and year to year. The extent of these regimes may be defined simply through the non-dimensional parameter h_c/h_m; the ratio of the spring-time critical layer depth to the winter mixed layer depth.

The key inferences from the idealized, two-layer model of DFMG (which is briefly outlined in the Appendix) are summarized in Figure 2, showing the sensitivity of the mean spring chlorophyll concentration to the mean spring vertical mixing rate in the seasonal boundary layer. The latter is related to the frequency and vigor of passing weather systems. We show results for finite ranges of h_c/h_m since it is advantageous (for the analysis of limited observed data) to examine these broad bio-physical regimes. In the left hand panel, the bounding curves are the solutions for $h_c/h_m = 0.05$ and $h_c/h_m = 0.4$. The shaded area represents the solutions for all values between. Thus the shaded region indicates a range of solutions which exhibit broadly common behavior in this parameter space. Likewise with the right hand panel, where the bounding curves are for $h_c/h_m = 0.6$ and 0.95. The figure illustrates the two qualitatively very different regimes, characterized by the parameter h_c/h_m. In regions where h_c/h_m is high (Fig. 2b), such as in the subtropics, an increase in bloom-period boundary layer mixing from one year to the next leads to a stronger bloom, due to enhanced nutrient supply where light is not limiting. In regions where h_c/h_m is low, such as the subpolar gyre, an increase of springtime vertical mixing can lead to a reduced bloom, as the phytoplankton are mixed below the critical depth and are light limited. Figure 2 illustrates the strongly contrasting responses of bloom period chlorophyll, in the two regimes, to changes in bloom period mixing.

The qualitative projections of the simplified model were borne out in a more complex, three-dimensional physical-biological model in DFMG. In this manuscript we use this framework to seek the suggested relationships between the spatial and temporal variability of the spring bloom and vertical mixing in the upper ocean in observed remote and *in situ* data. We examine *in situ* chlorophyll from Bermuda Atlantic Time Series (BATS - see for example, Michaels et al.(1994) and references therein) and Ocean Weather Station "India" (Williams and Robinson, 1973), and chlorophyll estimates derived from SeaWiFS remote ocean color observations. We infer vertical mixing in the ocean surface boundary layer from meteorological re-analysed products (air-sea heat flux and wind stress from NCEP re-analysis; (Kalnay et al., 1996)) and using bulk mixed-layer theory (Kraus and Turner, 1967).

In the following section we define the framework of the North Atlantic data analysis and describe the climatological values of the important parameters.

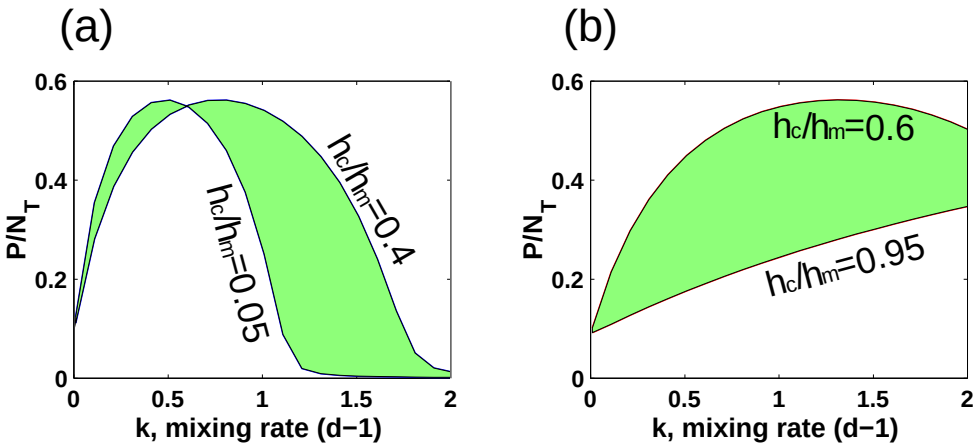

Fig. 2. Bloom period mean surface phytoplankton concentrations, normalized by winter mixed layer nutrient concentration (P/N_T), as a function of the spring-time vertical mixing rate within the seasonal boundary layer, κ from the idealized, two-layer, bio-physical model (see Appendix and Dutkiewicz et al., 2001). Solid lines indicate the solutions for the values of h_c/h_m bounding the regimes of interest. Shaded areas indicate all possible solutions within those regimes. (a) low h_c/h_m ratios ("subpolar" regime) and (b) high h_c/h_m ("subtropical"). The figure illustrates the predicted qualitative difference in chlorophyll in response to regional or interannual changes in spring time mixing. The broad, shaded swaths indicated the predicted spread of data for these broad classes of h_c/h_m. The values for μ, N_o and β are 1.5 d^{-1}, 0.1 μM and 0.5 d^{-1}, respectively for these experiments.

Section 2.2 outlines the methodology to infer vertical mixing rates in the upper ocean from meteorological information. In section 3 we examine the relationships between meteorological forcing, vertical mixing and the amplitude of the spring bloom, highlighting regional and interannual contrasts. In section 4 we discuss the results in a wider context and indicate the potential for future studies.

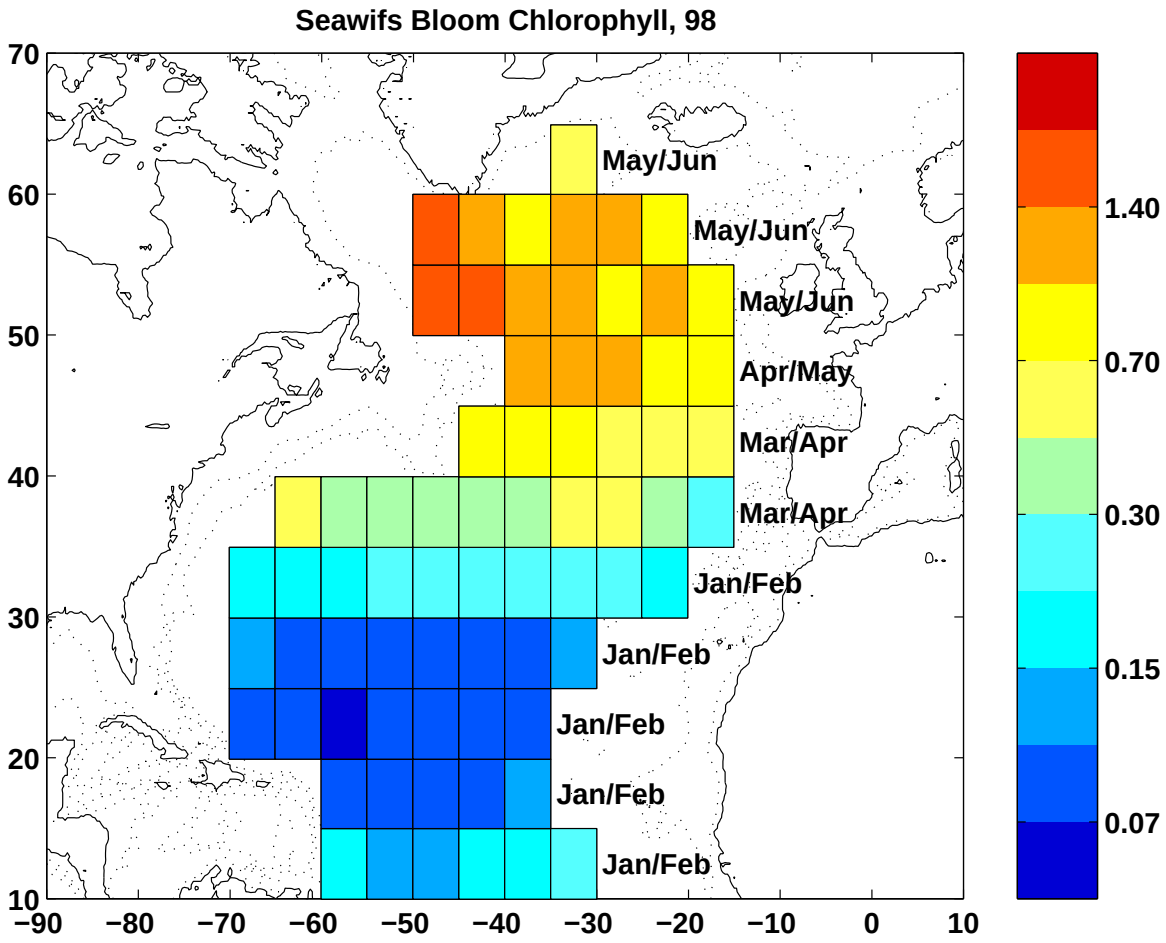

Fig. 3. Bloom-period (1998), SeaWiFS surface chlorophyll (mg/m^3) averaged in 5^o $\times 5^o$ bins. The months defined as the bloom-period (see text) are indicated for each latitude band.

2 Data Analysis Procedure.

Here we focus upon large scale variability in the open ocean of the North Atlantic. To filter the smaller scales (e.g. mesoscale features), we bin the biological and meteorological data into $5^o \times 5^o$ regions. The bins we choose, shown in Figure 3, are restricted to the open ocean with depth greater than 1000m. We do not address coastal areas which may be affected by many more complex factors, such as riverine nutrient sources and mixing to the sea floor. We also average the data over a two month period bracketing the bloom. We choose the bracketing period based on the timing in zonally averaged SeaWiFS, CZCS, and *in situ* data of the peak chlorophyll concentrations. The "bloom period", for the purposes of this analysis, occurs in January and February for much of the subtropical gyre. There is a sharp transition across the Gulf Stream and the spring bloom occurs as late as May and June to the south of Iceland.

Figure 3 shows the 1998 Level 3 (version 3) SeaWiFS chlorophyll data from these bloom months (noted on the figure), averaged over the $5^o \times 5^o$ bins. The chlorophyll distribution for the 1998 bloom exhibits the expected patterns over the basin with low surface chlorophyll concentrations in the oligotrophic subtropics and high concentrations in the subpolar gyre.

2.1 Climatological h_c/h_m.

We classify regional regimes of similar bio-physical characteristics with ranges of the parameter h_c/h_m; the ratio of the bloom period critical depth and the end of winter mixed layer. We estimate the broad distribution of this parameter using climatological data.

Critical Depth

Sverdrup (1953) defined the term "critical depth" as the depth above which integrated phytoplankton growth matched, or outweighed, mortality. This cannot be determined directly from remote observations. Various authors (Riley, 1947; Townsend et al., 1994; Hitchcock and Smayda, 1977) have defined a practical indicators of the critical depth to be that at which the vertically averaged flux of photosynthetically active radiation (PAR) is reduced to 21 W m^{-2}. The depth averaged light flux, E^*, over depth z, is estimated here from

$$E^*(z) = \frac{1}{kz} E_o e^{-kz}(1 - e^{-kz})$$

using a uniform attenuation coefficient, $k = 0.1$. We use a $1^o \times 1^o$ climatology of surface incident PAR, E_o, estimated using a radiative transfer model by Watson Gregg (personal communication). This depth is estimated for each of the bins, averaged over the bloom period, as shown in Figure 4(a). The critical depth, estimated in this way, varies between 20m and 60m, and is generally deeper in the subtropics due to the stronger incident flux.

Winter Mixed Layer Depth.

We define the end of winter mixed layer depth to be the average depth during the two months immediately preceding the bloom period. We estimate the mixed layer to be where the potential density differs from the surface density by less than 0.125 σ_θ units. Density is taken from Levitus monthly climatology (Levitus and Boyer, 1994). We average over the two month "end of winter" period and within the $5^o \times 5^o$ bins (Fig. 4b). As may be anticipated, the mixed layer depth is shallow (less than 100 m) over most of the subtropics and considerably deeper (greater than 300 m) in the subpolar gyre.

The ratio h_c/h_m is mapped in Figure 4(c). The broad regional variations are dominated by gradients in the winter mixed layer depth. The subpolar regions are characterized by low values; subtropical regions have much higher values. Some tropical areas have $h_c/h_m > 1$, suggestive of a year-round submerged chlorophyll maximum. These areas cannot be described by the idealized two-layer model (Appendix) considered here and, as such, are excluded from this analysis.

2.2 Ocean Boundary Layer Mixing Rates and Surface Forcing.

Our goal is to relate variability in bloom period chlorophyll to changes in climate and weather patterns in the atmosphere, mediated by meteorologically induced changes in vertical mixing within the seasonal boundary layer of the ocean. The simple two-layer description of the system (Appendix and DFMG) described the vertical mixing using a simple rate constant, κ. Such a rate constant is easily diagnosed from a numerical general circulation model where mixing is parameterized either as convective adjustment due to static instability or as a turbulent diffusion (e.g. DFMG). In this examination of remote and *in situ* observations, however, such a mixing rate constant is more difficult to evaluate.

Here we apply concepts from bulk mixed-layer models to link surface forcing and ocean boundary layer mixing. Vertical stirring of properties in the boundary layer is related to the rate of generation of turbulent kinetic energy (TKE). Bulk mixed layer theories (Kraus and Turner, 1967; Niiler and Kraus, 1977), assuming that the mixed-layer is vertically homogeneous, relate the generation of TKE in the ocean boundary layer to wind stirring and buoyancy forcing in the following way:

$$\int_h^o \frac{d(TKE)}{dt} = m_1 u_*^3 + m_2 \frac{\alpha g}{\rho c_p} \frac{h}{2} H_o \qquad (1)$$

where h is the mixed layer depth, $u_* = \sqrt{\frac{|\vec{\tau}|}{\rho_o}}$ is the wind induced friction velocity, $\vec{\tau}$ is the wind stress, and ρ_o is water density. The total air-sea heat flux, H_o, includes contributions from sensible and latent heat exchange, and long and shortwave radiative fluxes. The coefficients m_1 and m_2 are difficult to evaluate and are probably not constant (Kraus, 1988); however many authors (e.g. Kraus et al., 1988) have assumed $m_1 = 1.25$ and $m_2 = 1$ for negative buoyancy forcing (i.e. heat loss from the surface ocean) and $m_2 = 0.2$ for positive buoyancy forcing. Further effects of penetrative radiation, internal waves, freshwater fluxes and dissipation have been neglected for clarity.

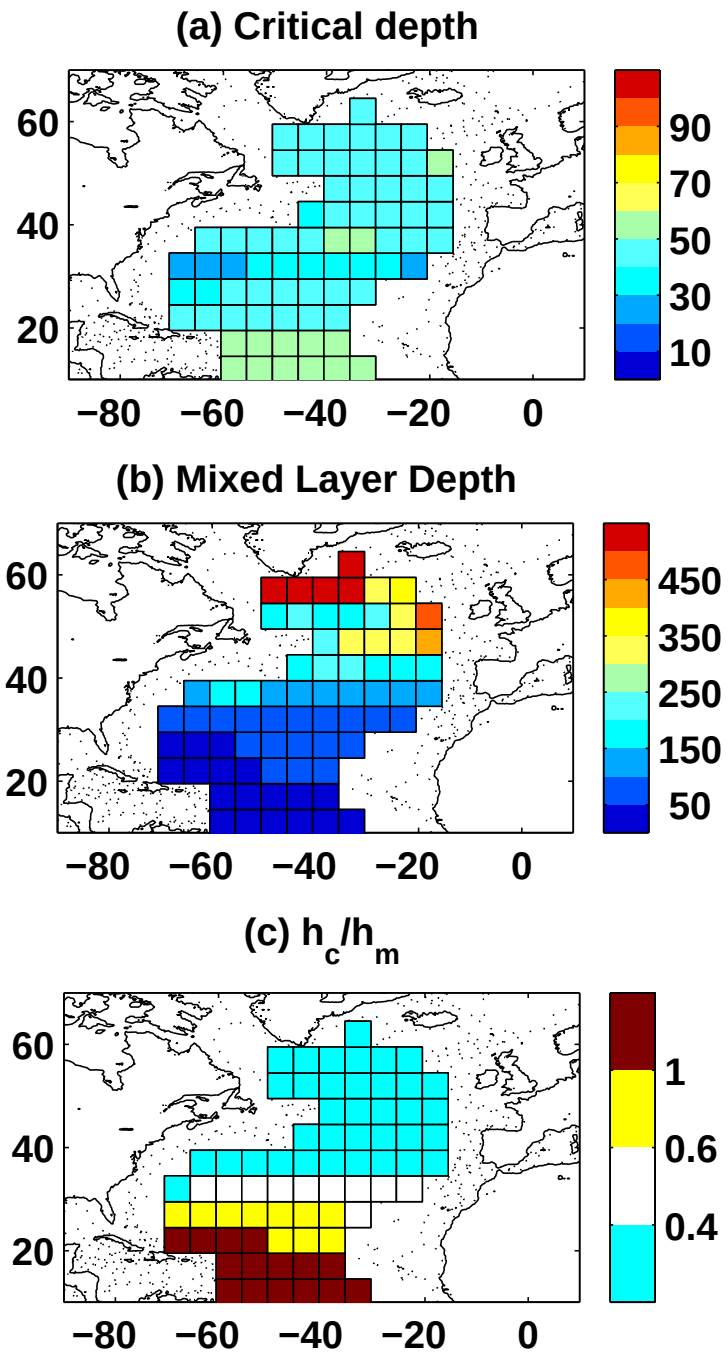

Fig. 4. Climatological: (a) h_c, spring critical layer depth (m); (b) h_m, end of winter mixed layer depth (m); (c) h_c/h_m.

The action of the wind always increases the TKE in the boundary layer (first term on right in Eq. 1). Buoyancy forcing can either reduce TKE, when the water column is stratifying due to an input of heat to the surface ocean ($H_o < 0$), or increase TKE when the water column is cooled from above ($H_o > 0$).

To estimate the rate of TKE generation in the mixed layer using Eq. (1) we

require estimates of air-sea heat exchange, H_o, friction velocity, u_*, and mixed-layer depth, h. The first two may be obtained from re-analysed meteorological products (e.g. NCEP; Kalnay et al., 1996). Mixed layer depth may be estimated from hydrographic data; either *in situ* profiles at the time-series' sites, or from gridded climatology.

Figure 5 shows the mean bloom-period air-sea heat flux in 1998 derived from NCEP re-analysis data. In general, areas of low h_c/h_m are characterized by negative heat flux during the spring bloom (heat gain by the surface ocean) since the bloom occurs when the water column stabilizes (Sverdrup, 1953). In regions of high h_c/h_m, the bloom occurs while the seasonal boundary layer is still unstable, the air-sea heat flux is still positive (out of the ocean) and mixed-layer depths are close to their annual maximum (Menzel and Ryther, 1961).

3 Relating Observed Chlorophyll and Meteorological Forcing.

Here we examine *in situ* time-series and remote observations of chlorophyll variability in both time and space. Our analysis is guided by the idealized two-layer model discussed in Section 1 and in the Appendix. We seek, in the observed data, the relationships between chlorophyll and meteorological parameters (mediated by vertical mixing) suggested by the simple model and indicated in Figure 2. We will examine the observations within the framework laid out above, sorting the data according to bio-physical regimes guided by the local value of h_c/h_m.

Time-series observations at the Bermuda Atlantic Time-Series Station (BATS, subtropical, 32^{o}N, 65^{o}W) and Ocean Weather Station "India" (OWS "I", subpolar, 59^{o}N, 19^{o}W) are examined in terms of local, interannual changes in the bloom, but cannot provide information about the larger scale spatial patterns. Remote ocean color observations, from SeaWiFS, enables us to consider both regional variability of the bloom period and interannual changes.

3.1 Interannual Variability of In Situ *Data: BATS and OWS "I"*

The observed time series of chlorophyll in the upper 10m at BATS is shown in Figure 6(a) for the period 1990 to 1996. Here the bloom occurs early in the year, usually January and February, but the timing and, in particular, the amplitude of the bloom exhibit significant interannual variability. In Figure 6(b) we plot the mean bloom-period chlorophyll concentration for each year against the corresponding total air-sea heat flux, H_o (positive defined as heat

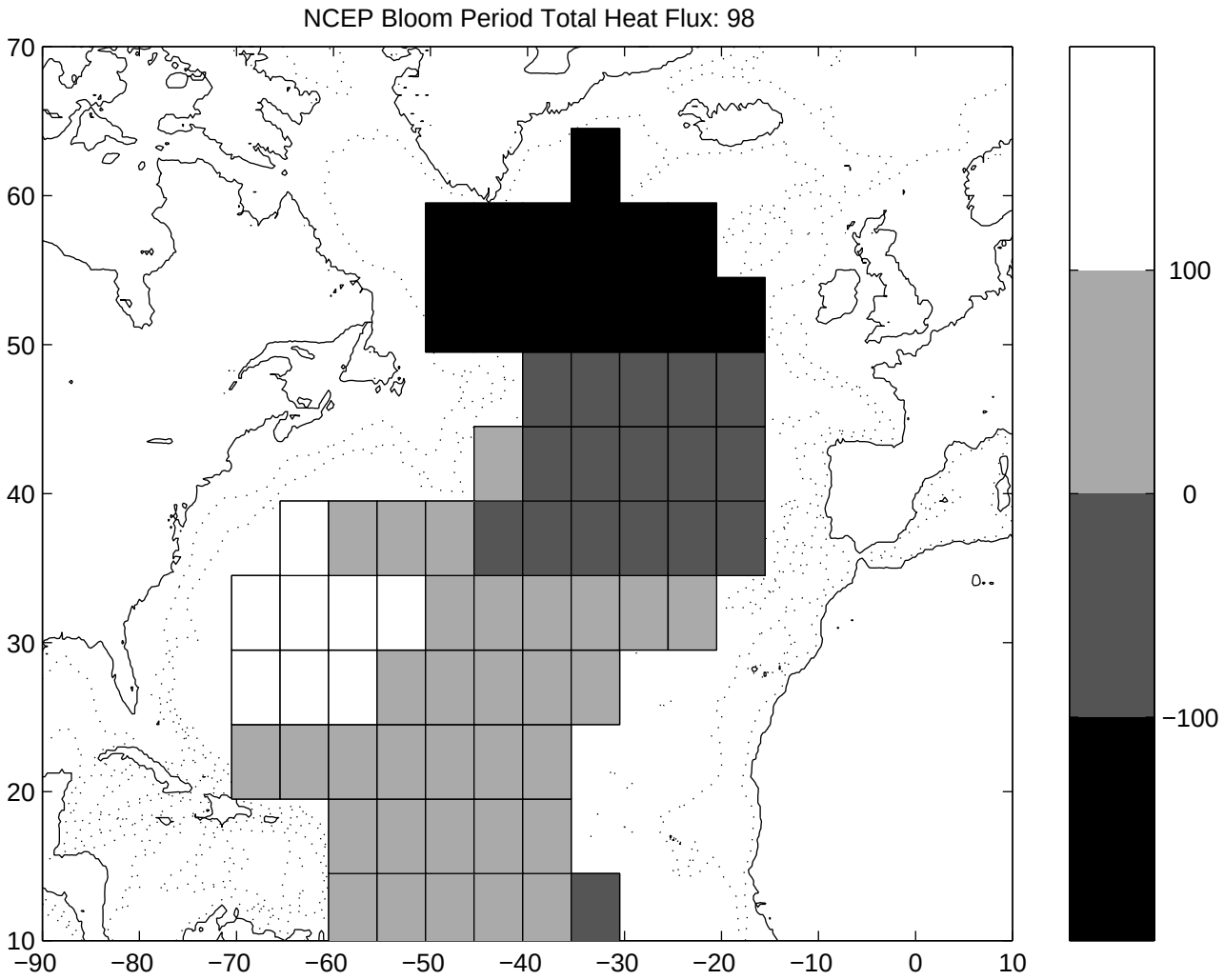

Fig. 5. Total air-sea heat flux for the 1998 bloom period (W/m^2, positive out of the ocean). Data from NCEP re-analysis, are averaged for the bloom period as defined in Figure 3. The total heat flux includes contributions from sensible and latent heat exchanges, along with long and short wave radiative fluxes. The subtropical gyre is losing heat and unstable during its bloom, while the subpolar gyre is gaining heat and restratifying.

loss from ocean), and friction velocity cubed, u_*^3. The physical parameters are derived from NCEP re-analysis products and represent the forcing terms that induce vertical mixing. In addition, we plot the chlorophyll against mixed-layer TKE generation (see Eq. 1) using estimates of h from the time-series hydrographic data. In each panel, vertical mixing in the boundary layer increases to the right. The bloom in the Sargasso Sea occurs during the period of active heat loss and entrainment (Menzel and Ryther, 1961). At this site the wind stirring and heat forcing effects on mixing and chlorophyll reinforce one another.

Bermuda is in the high h_c/h_m regime, and increased mixing during the bloom

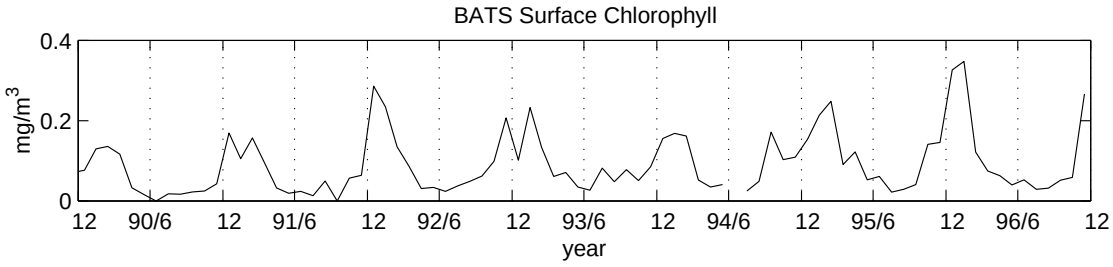

(a)

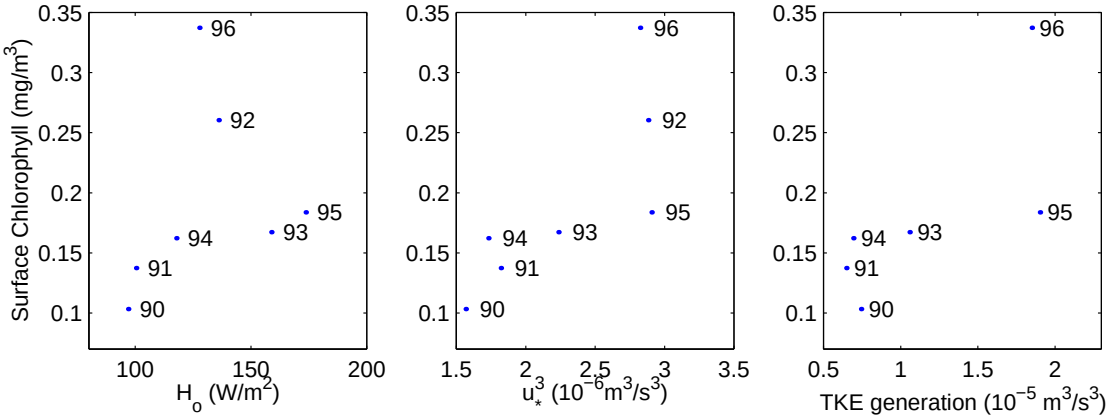

(b)

Fig. 6. (a) Bermuda Atlantic Time-Series (BATS) upper 10m chlorophyll concentration (mg/m^3) from 1990 to 1996; (b) Scatter plots of bloom-period, upper 10m chlorophyll against total heat air-sea heat flux, H_o; friction velocity cubed and TKE generation (Eq. 1). All data are averaged over January and February for each year (1990 to 1996). Mixed layer depths for Eq. 1 are determined from *in situ* density measurements.

leads to a stronger bloom with higher chlorophyll concentrations. In all three panels of Figure 6(b), there is a general trend of greater mean spring chlorophyll concentrations associated with stronger mixing supply in the boundary layer and enhanced nutrient supply. The positive gradient suggested in the data (Fig. 6b) is qualitatively consistent with the gradient suggested in Figure 2 for the high h_c/h_m, low mixing rate regime appropriate for the Sargasso Sea. While there is a qualitative agreement of the model with the data there is significant scatter in the plots. Fitting a linear relationship to the data in the right hand panel (chlorophyll/TKE generation), we find a positive correlation, as predicted, with $r^2 = 0.55$, suggesting that a significant fraction of the interannual variability of the bloom may be attributed to changes in meteorological forcing. The scatter indicates processes not represented in the simple model and uncertainties in the data. Several studies have demonstrated evidence of a significant contribution to annual new production due to rectified nutrient pumping by mesoscale eddies (McGillicuddy et al., 1998). The passage of an eddy could cause significant departures from the local one-dimensional springtime balance. For instance, the bloom of 1996 stands out as particularly strong, relative to the wind and heat flux forcing (Fig. 6b). An eddy feature passed through the region towards the end of the bloom period (personal communication, Dennis McGillicuddy) and may have contributed to the anomalously strong bloom.

The idealized model suggests a very different response to interannual changes in boundary layer mixing in low h_c/h_m (subpolar) regimes. Here light limitation and restratification effects become important (Sverdrup, 1953). Time-series observations of chlorophyll in the subpolar regions of the North Atlantic are few. We examine the data collected at OWS "India" between 1971 and 1975. Chlorophyll concentrations (Fig. 7a) and mixed layer depth were measured only in spring and summer. Additionally, because of a gap in hydrographic observations from which to determine mixed-layer depth, we do not estimate TKE generation rates in the bloom of 1973.

We plot the surface, bloom-period chlorophyll at OWS "I" against NCEP derived H_o, u_*^3 and TKE generation in Figure 7(b). The bloom occurs during a period of ocean heat gain and restratification (Sverdrup, 1953). The heat flux term in Eq. (1), dominates the changes in TKE during the months of the bloom. The data set does not show a clear trend between the interannual variation of the bloom and meteorological forcing. There are several possible explanations: There may simply be too little, and too sparse, data to reveal the relationships expected from the model (Fig. 2). Alternatively, sources of variability which were not built into the idealized model (e.g. unresolved ecosystem processes, mesoscale motions, variability of incident PAR) may dominate the variability in the bloom here, outweighing the effect of local meteorological forcing. This issue is discussed further in relation to the remotely observed data.

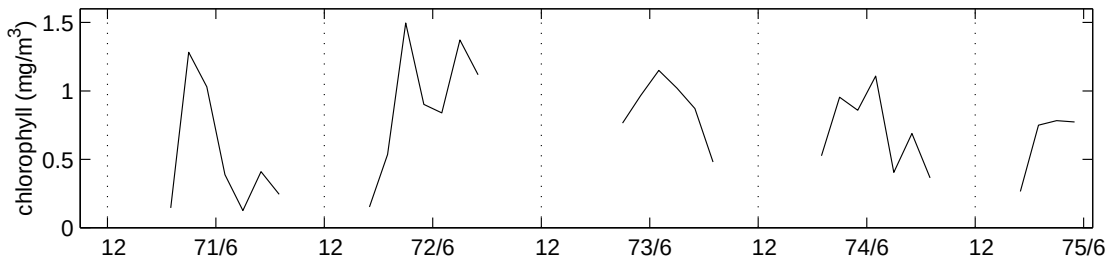

(a)

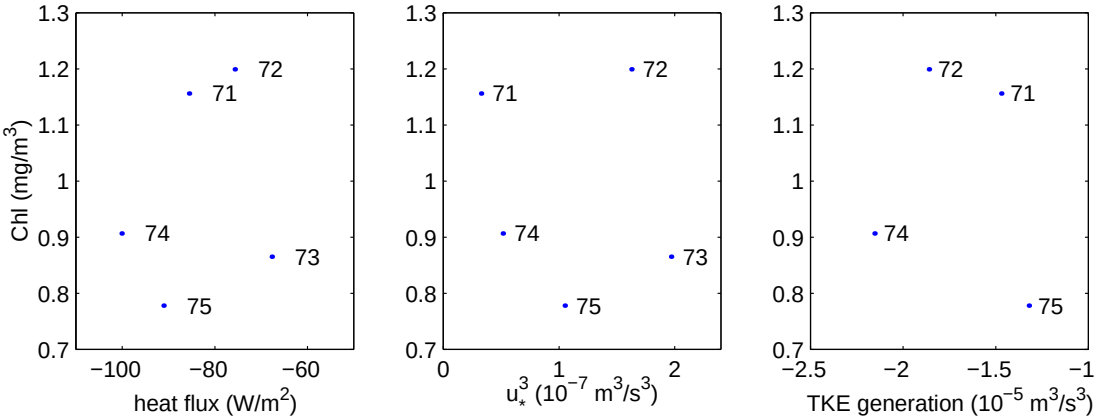

(b)

Fig. 7. (a) OWS "India" upper 10m chlorophyll concentration (mg/m^3). (b) Scatter plots of OWS "I" upper 10m chlorophyll against total air-sea heat flux, H_o; friction velocity cubed; and TKE generation (Eq. 1). All data are averaged over May and June for each year (1971 to 1975). Mixed layer depths for Eq. 1 are determined from *in situ* temperature measurements. Hydrography and mixed layer depth are unavailable for 1973, precluding an estimate of TKE generation for that bloom.

The analysis of the *in situ* data sets illustrates how we may use this framework to seek to understand the physical-biological mechanisms at play in the North Atlantic ocean. We are, however, limited by the difficulty of obtaining data with reasonable spatial and temporal coverage. The advent of high density, high quality, remote observations of ocean color and derived chlorophyll provides an excellent opportunity for a more comprehensive analysis.

3.2 Regional Controls: SeaWiFS Spring 1998

To examine the role of variations of physical forcing between and within the broad biophysical regimes we first consider the relationship of SeaWiFS chlorophyll to the physical forcing variables during the bloom period of 1998. We plot the bloom-period mean of the 8-day Level 3, composite data, for each 5^o

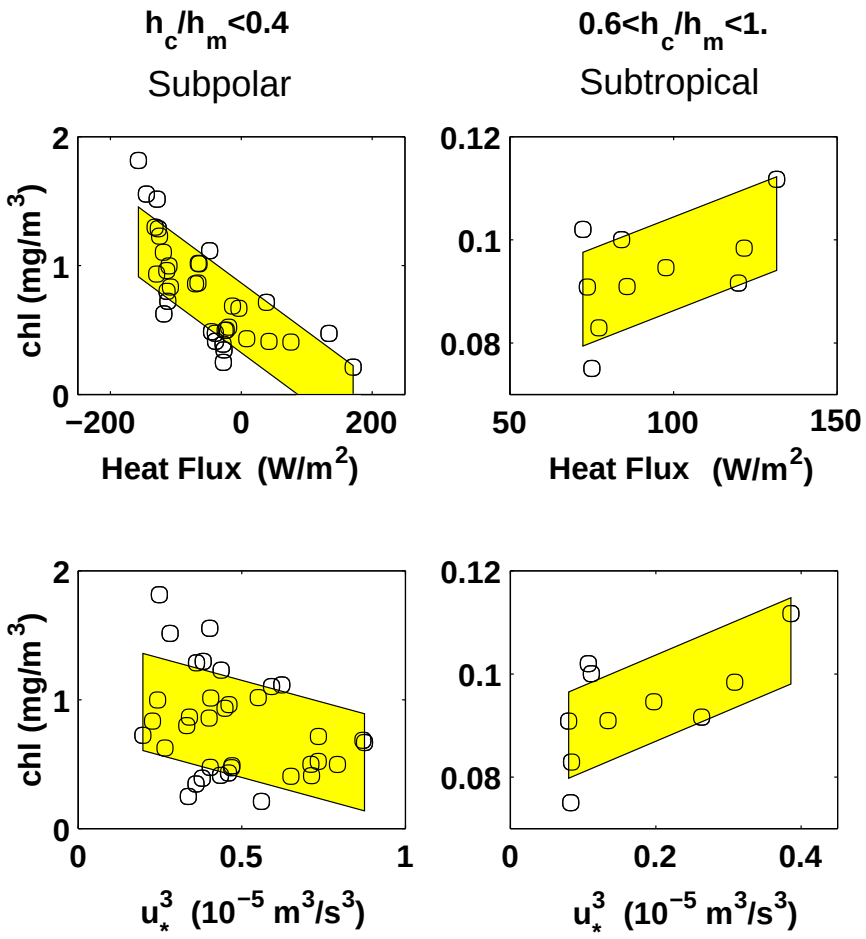

Fig. 8. Bloom Period (1998) SeaWiFS chlorophyll (mg/m^3) plotted against NCEP total heat flux (W/m^2) and friction velocity, u_*^3 ($\times 10^{-6}$ m^3/s^3) derived from NCEP wind stress data. Each data point indicates the 1998 "bloom" average for one five degree bin (Fig. 3). We separate the results into subpolar and subtropical regimes according to broad classes of the local value of h_c/h_m (ranges indicated above figure). Left column shows results for the small h_c/h_m, subpolar regime; the right column shows results for the high h_c/h_m, subtropical regime. The shaded regions indicate one standard deviation either side of a linear least squares fit (see text for discussion).

$\times$ 5^o bin, against the NCEP re-analyzed H_o and u_*^3, averaged over the same bins and time period (Fig. 8).

The simple theory, illustrated in Figure 2, suggests qualitatively very different responses to increased boundary layer mixing for regimes of small and large h_c/h_m (i.e. subpolar and subtropical). We group the data by their physical-biological regime, according to the classes illustrated in Figure 2, in order to reveal how the large-scale, regional variations in chlorophyll, during this one spring, depend upon regional variations in the weather. We choose the same broad classes of h_c/h_m as depicted in Fig. 2 in order to maximize the number of data points per class, but restrict the classes enough to maintain

the distinct regional characteristics. The limiting ranges of these classes are somewhat subjective, but the relationships elicited are robust for reasonable choices. Here we choose the regimes to be h_c/h_m <0.4 (subpolar); and 0.6< h_c/h_m <1. (subtropical). We do not consider the regime $0.4 < h_c/h_m < 0.6$, as it straddles the subtropical and subpolar regimes and there is no clear sensitivity in the model. The regime where $h_c/h_m > 1$ suggests a permanent sub-surface chlorophyll maximum which is not described by the simple theory or examined here.

While we do not plot explicit error bars on the data points, it should be noted that remote chlorophyll estimates have an uncertainty of, at best, a few percent and further uncertainty is introduced by missing data and compositing. Meteorological re-analysis products are subject to similar uncertainties. Here we do not normalize the chlorophyll concentrations by local, winter mixed layer nutrient concentrations. Estimating winter nutrient concentrations derived from climatology (Williams and Follows, 1998) does not lead to a significant change in the broad relationship between chlorophyll and mixing at high latitudes since light limitation is the controlling factor. In addition, estimating the interannual variability in the nutrient concentration introduces significant additional uncertainty to the relationships.

Subpolar, $h_c/h_m < 0.4$**:**

Data from the subpolar regime are depicted in the two left panels of Figure 8. Chlorophyll concentrations decrease with increasing heat loss from the ocean surface (upper left panel). In some parts of this region, the time averaged air-sea heat flux is destratifying (H_o positive), indicating episodes of vigorous stirring of the boundary layer. Here chlorophyll concentrations remain low and the bloom is retarded. Due to the broad, latitudinal classification of the bloom period, some of these areas may still be in "pre-bloom" conditions. Other such areas, however, have experienced intermittent stratification, blooming and mixing (Stramska et al., 1995). Where the water column is stratifying (H_o negative) the bloom shows a clear trend of increased chlorophyll with increased heat gain (stratification). There is no clear relationship between u_*^3 and the surface chlorophyll (lower left panel). During the bloom period in the subpolar region ($h_c/h_m << 1$), wind-stirring acts to de-stratify the water column while buoyancy forcing attempts to stratify the water column. The bloom is enabled when the latter dominates and restratification occurs. Hence, in this region, bloom period chlorophyll is closely related to the buoyancy forcing, H_o, but has little or no relationship to the wind-stirring.

Subtropical, $0.6 < h_c/h_m < 1.0$**:**

In contrast, in the subtropics, the bloom is enabled by entrainment of nutrients during mixed-layer deepening. Wind stirring and buoyancy forcing terms act

in concert and both can influence the vigor of the bloom. In the subtropical panels of Figure 8 (right hand panels) there is clear positive correspondence between chlorophyll and both surface heat loss and wind speed. The air-sea heat flux is positive (i.e. destratifying) during the bloom period. Contributions to TKE generation from the wind and buoyancy forcing work together. In this region the wind-stirring effect may dominate the mixing and control the bloom.

Both subpolar and subtropical data are overlain by a shaded swath representing an area one standard deviation on each side of the best linear fit to the data as plotted. Since we have plotted broad classes of h_c/h_m, in order to maximize the available data in each class, we do not expect the data to fall in a tight line, rather on a swath, reminiscent of the areas bracketed by the bounding model solutions in Figure 2. Even though fitting a simple linear relationship to the data is perhaps over simplistic, especially with these broad classes of h_c/h_m, it shows in Figure 8 a significant connection between the physical and biological variations. For the subpolar region chlorophyll and heat flux (upper left panel) the best linear fit gives $r^2 = 0.54$. More significantly, the slope of the linear fit is negative, and the spread of the data relative to the best fit line (indicated by the the shaded swath) is comparable to the spread predicted by the simple model for a broad class of h_c/h_m (compare Figure 2). The subpolar region does not show a significant relationship with the friction velocity ($r^2 = 0.10$) because the bloom is dominated by the processes which aid restratification. The relationship between subtropical chlorophyll and friction velocity (bottom right panel) is examined similarly. The linear fit has a positive gradient (as predicted) and $r^2 = 0.42$. Again, the width of the shaded swath is consistent with our expectation due to the breadth of h_c/h_m class (compare Figure 2). The subtropical data also shows a positive gradient with respect to heat flux (upper right panel) but a weaker connection ($r^2 = 0.30$). These linear relations provide a simple quantification of the connections between the physical and biological data. However given the broad classes of h_c/h_m gathered in the data, these linear relationships do not provide a full account of the influence of the meteorological forcing on the bloom. A more robust quantification is possible for local, interannual time-series', where h_c/h_m classes are more restricted (see Sections 3.1 and 3.3).

We summarize the subpolar and subtropical regimes in Figure 9, plotting bloom mean chlorophyll against TKE generation rates (following Eq. 1), and using diagnostic, climatological, mixed-layer depths, h. Added uncertainty is introduced through this estimation, along with the two estimated coefficients m_1 and m_2. However, comparing Figures 9 and 2, we find that the observed data generally support the dependencies suggested by the simplified model (c.f. Fig. 2). The qualitative regional changes within regimes are consistent between the model and observations.

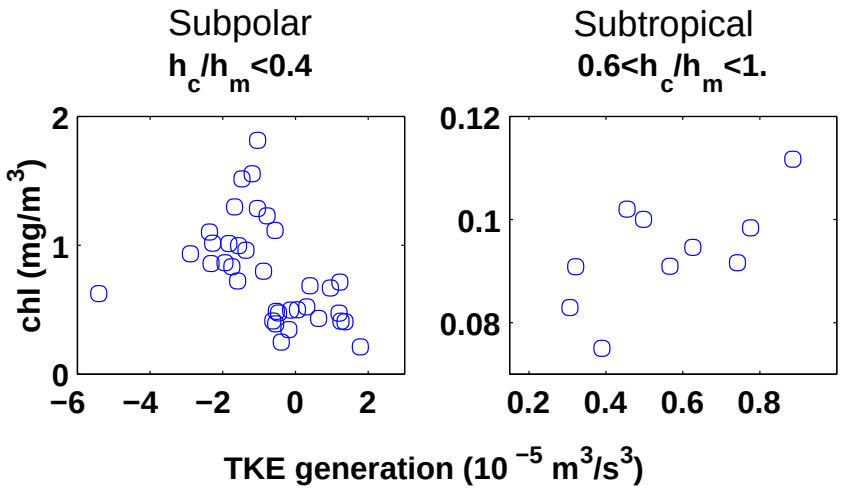

Fig. 9. Regional variability in the spring bloom. Bloom Period (1998) SeaWiFS chlorophyll (mg/m^3), plotted against TKE generation (derived using equation (1) and monthly, climatological mixed layer depth h). Data grouped by broad h_c/h_m classes reflecting the subpolar (low h_c/h_m) and subtropical (high h_c/h_m) regimes. The h_c/h_m classes are defined above the figure. Generation of TKE is assumed to be proportional to the rate of vertical mixing within the seasonal boundary layer. Compare the trends and spread in the data with the idealized model results in Figure 2.

3.3 Interannual Changes: SeaWiFS 1998, 1999 and 2000.

In the previous section, we demonstrated that regional variations in a single year's spring bloom are consistent with a simple relationship to regional variations in meteorological forcing. Can we begin to interpret observed interannual

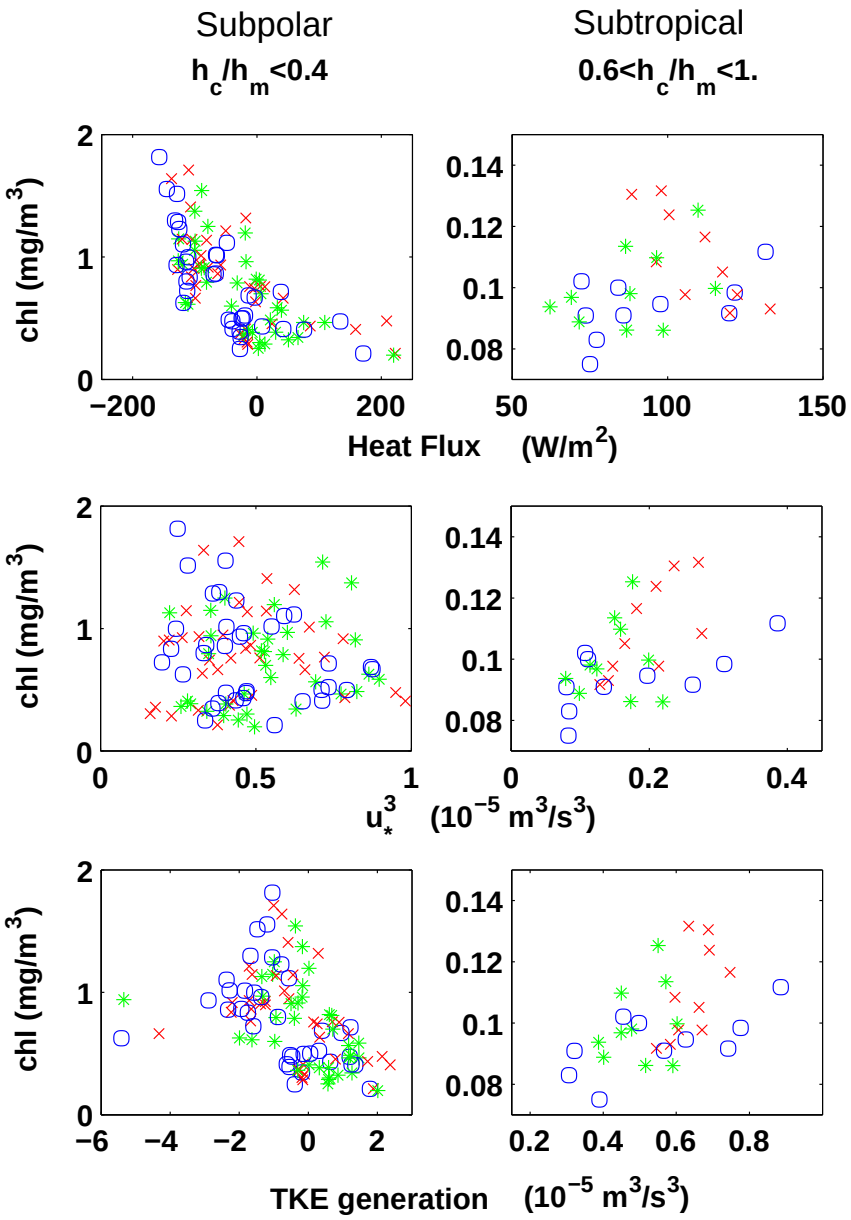

Fig. 10. Interannual and regional variability in the bloom. SeaWiFS level 3 chlorophyll (mg/m^3) for each of the three blooms observed to date (1998 o, 1999 x, 2000, $*$) plotted against (upper panel) heat flux (W/m^2); (middle panel) friction velocity, u$_*^3$ ($\times 10^{-5}$ m^3/s^3); and (lower panel) generation of TKE ($\times 10^{-5}$ m$^3/s^3$), derived using (1). Low (subpolar) and high (subtropical) h_c/h_m regimes are shown. Data are averaged over the bloom period and for the five-degree bins depicted in Figure 3. Compare the trends and spread of data in the lower panels to the idealized model results in Figure 2.

differences in remotely observed chlorophyll in the same way? To date, three complete "bloom" periods have been observed using SeaWiFS: 1998, 1999 and 2000.

In Figure 10 we plot the SeaWiFS chlorophyll against u_*^3, H_o and the TKE generation for all three blooms, in the low and high h_c/h_m regimes. The figure shows the same information as Figures 8 and 9 but for years 1999 and 2000 in addition to 1998. Here we focus on interannual change. Each annual bloom shows regional variations similar to those of 1998, reinforcing the general observation of contrasting sensitivity in each gyre to changes in mixing (lowest panels). In each year the regional patterns in the subpolar bloom show a close relationship to surface heat fluxes, while in the subtropics, wind-stirring appears to dominate the overall regional variations, though both wind and buoyancy forcing contribute significantly to TKE generation. For example, in 1999, the subtropical chlorophyll shows a negative correlation to the surface heat flux, but has a positive correlation with both u_*^3 and TKE generation. The three outlying data points in the lower left panel are from the northernmost bin between Iceland and Greenland suggesting the possibility of a different controlling mechanism there, perhaps due to strong currents and advective influences.

We examine the data for interannual trends. In the high h_c/h_m regime (subtropics), there are apparent, co-ordinated interannual variations on the large scale, following the general trend of higher chlorophyll with increased TKE (for example, compare 1999 and 2000 in the lower right panel). There is no discernible interannual separation in the low h_c/h_m regime, however. This subtropical-subpolar contrast is consistent with the visual impression from Figure 1, and also the studies of Fuentes et al.(2000) and Uz et al.(2001) who demonstrate a polewards decrease in scales of spatial variability in SeaWiFS chlorophyll, consistent with changes in the radius of deformation.

The slopes and spread of the data are consistent with the swathes in Figure 2 which represent the solutions for broad classes of h_c/h_m. Making simple, linear fits to the data (again, over simplistic for such broad classes of h_c/h_m) we find a statistically significant negative slope for the general subpolar chlorophyll/heat flux relationship, and positive slopes for the general subtropical chlorophyll/heat flux and chlorophyll/friction velocity relationship. The signs of the slopes (for a linear fit) are robust at the 95% confidence level.

We emphasize the contrast of interannual variability in the subpolar and subtropical regimes in Figure 11. Here, for the two h_c/h_m regimes we display the bloom period chlorophyll data as a function of TKE generation. Here we emphasize the local interannual variability, joining each set of three points from the same $5^o \times 5^o$ bin. The trajectories run from the year with lowest bloom-time TKE generation and end at the year with highest. The subtropical regime shows strong and consistent patterns of interannual change through the whole region. Each individual bin exhibits a positive correlation between bloom-period chlorophyll and meteorologically induced vertical mixing, consistent with the time-series data from Bermuda (Fig. 6b). In the subtropics,

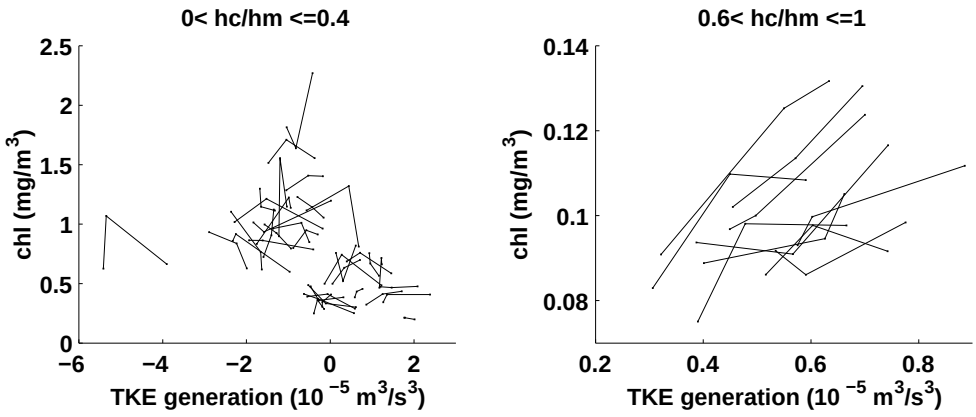

Fig. 11. Interannual trajectories. Annual bloom data points for each of the three observed blooms (1998, 1999, 2000) in each five-degree bin are shown. Lines join each set of three bloom data points from the same geographic bin, starting at the data point with the lowest generation of TKE and proceeding with increasing TKE generation. The left panel shows the subpolar regime, the right panel the subtropical. The subtropical regime shows clear and consistent interannual trends with stronger mixing leading to a stronger bloom. Interannual changes are of the same order as regional variations within the subtropics. The subpolar regime shows no clear interannual trends, and variability is dominated by regional changes.

the local interannual changes are comparable in amplitude to the regional variations.

In the subtropical regime, we determine a simple linear fit to each of the three year time-series, each of which represents a narrow range of h_c/h_m. This analysis shows a strong and striking relationship between mixing and the bloom. Of the ten subtropical bins which have data for all three spring periods, nine have a statistically positive slope at the 95% confidence level, and of these, changes in mixing can account for greater than 75% of the variability.

In strong contrast, the subpolar trajectories are not coordinated and show no preferential direction. The amplitude of the interannual changes of chlorophyll and boundary layer mixing are small relative to the broad regional variations. The figure reinforces the view emerging from the OWS "I" data and previous depictions of the SeaWiFS data, that the local interannual variability in the subpolar gyre is weaker, though the broad regional changes are consistent with the strong change in surface heat flux, H_o. This may be because the subpolar bloom is controlled by the restratification process which is strongly influenced by small-scale baroclinic eddies (Jones and Marshall, 1997; Levy et al., 1998). In addition there is an absence of large scale pattern in spring and summer meteorological variability (compared to winter when the subtropical bloom occurs - see Discussion). Other potential influences include top-down control on the ecosystem, poorer data coverage at higher latitudes due to cloudiness, and variability in incident PAR due to changes in cloud cover (Townsend et al., 1994).

4 Summary and Discussion.

We have organized and examined observations of the North Atlantic spring bloom, from *in situ* time-series and SeaWiFS ocean color observations, using a framework suggested by an idealized, bio-physical model of the ocean's surface boundary layer. The model encapsulates subtropical ($h_c/h_m > 0.6$) and subpolar ($h_c/h_m < 0.4$) regimes which relate to those observed and previously discussed (Menzel and Ryther, 1961; Sverdrup, 1953). The model identifies regimes of contrasting bloom response and sensitivity to regional and interannual variability in meteorological forcing.

Using this framework, we have examined *in situ* time-series from BATS and OWS "India", in conjunction with re-analysised meteorological data from NCEP. We find a clear qualitative correspondence between the subtropical theory and observations of the spring bloom at BATS. At OWS "I", no clear relationship emerges in the record, perhaps due to the sparse data record and/or because of mechanisms of variability not accounted for in the simple model.

A regional analysis of the 1998 chlorophyll bloom, using data from SeaWiFS and NCEP, shows a clear correspondence with the theory: the *regional* variations of the bloom within the subtropical and subpolar regimes display opposite responses to enhanced, weather-induced, boundary layer mixing in the spring. The expected chlorophyll to mixing relationships emerge in both subtropics and subpolar regimes.

In the subtropics, local *interannual* changes conform to our expectations from the simple model also (both at BATS and in the locally binned SeaWiFS data). The region exhibits large-scale, coordinated, interannual changes in the bloom. This is not true in the subpolar regime, where the local interannual changes do not conform to the model (though the large-scale regional variations do). Here, no clear relationship to meteorological forcing emerges in the data, either at OWS "I" or in the binned SeaWiFS data.

Why does data show connections between the bloom and meteorological forcing in both regional and interannual variations in the subtropics, but only for regional changes in the subpolar gyre? There are, of course, potentially significant sources of variability not included in the simple model of Figure 2. These include lateral advection, the influence of mesoscale motions, changes in incident photosynthetically active radiation and ecological processes not described in the highly idealized model. Indeed, these processes must active to some degree, providing introducing sources of variability most likely uncorrelated with upper ocean mixing. In the subpolar regions, on local and interannual scales, they may dominate.

In a more complex three-dimensional circulation and ecological model, DFMG found that lateral advection does play an important role in controlling the bloom in some regions, even in a relatively coarse resolution model. In addition, high latitudes have characteristically smaller dynamical scales due to the changing Rossby radius, and this appears to be reflected in phytoplankton spatial decorrelation scales (Fuentes et al., 2000; Uz et al., 2001). In the subpolar regions, where the bloom is initiated by restratification, motions on the scale of the radius of deformation are imprinted on this process. We should expect a strong signature of meso-scale variability in the high latitude bloom. This has been demonstrated in high-resolution, three-dimensional numerical models of convection, restratification and biological productivity (Levy et al., 1998). In contrast, the subtropical bloom may be affected by eddies (see Section 3.1), but is largely controlled by the winter mixed-layer deepening and entrainment of nutrients.

Since local interannual changes in the strength of the subpolar bloom do not appear to be simply related to changes in the local meteorological forcing we believe that one or more of these other influences are dominant on the local, interannual scale. The subpolar regional signal in TKE generation and bloom chlorophyll is much stronger than the local interannual changes.

Outlook: Response to Shifting Regional Climate Regimes.

This analysis provides a useful framework for examining the connections between local meteorological forcing and the biological response on regional and interannual scales. Clearly this analysis is a qualitative one, given the simplifications and uncertainties in both the conceptual framework and the data sets available. However, we can use this framework to explore the connections between regional climate regimes and the biological response.

In Figure 12 we show the difference in winter and spring total air-sea heat flux and friction velocity cubed (u_*^3) between the decades of the 1990's and the 1960's, derived from NCEP re-analyzed fields. A significant fraction of regional climate variability in the North Atlantic may be characterized by the North Atlantic Oscillation (NAO Index) which is defined by the anomaly in sea-level pressure difference between Lisbon, Portugal and Iceland. The index exhibits variability over a broad range of timescales, from days to decades. A high NAO index period is generally characterized by a strong jet stream oriented towards the north, strong heat loss from the subpolar north-western Atlantic, and deeper winter convective mixing in that region. The western subtropical ocean experiences weaker than average winter-time heat loss and shallow winter mixing. The converse is true in low NAO index periods (Hurrell, 1995; Cayan, 1992). The 1990's were characterized by a high NAO index for much of the decade, while the opposite is true for the 1960's (Hurrell, 1995). The winter (Jan-Mar) heat flux difference echoes this, showing the classic tripole pattern

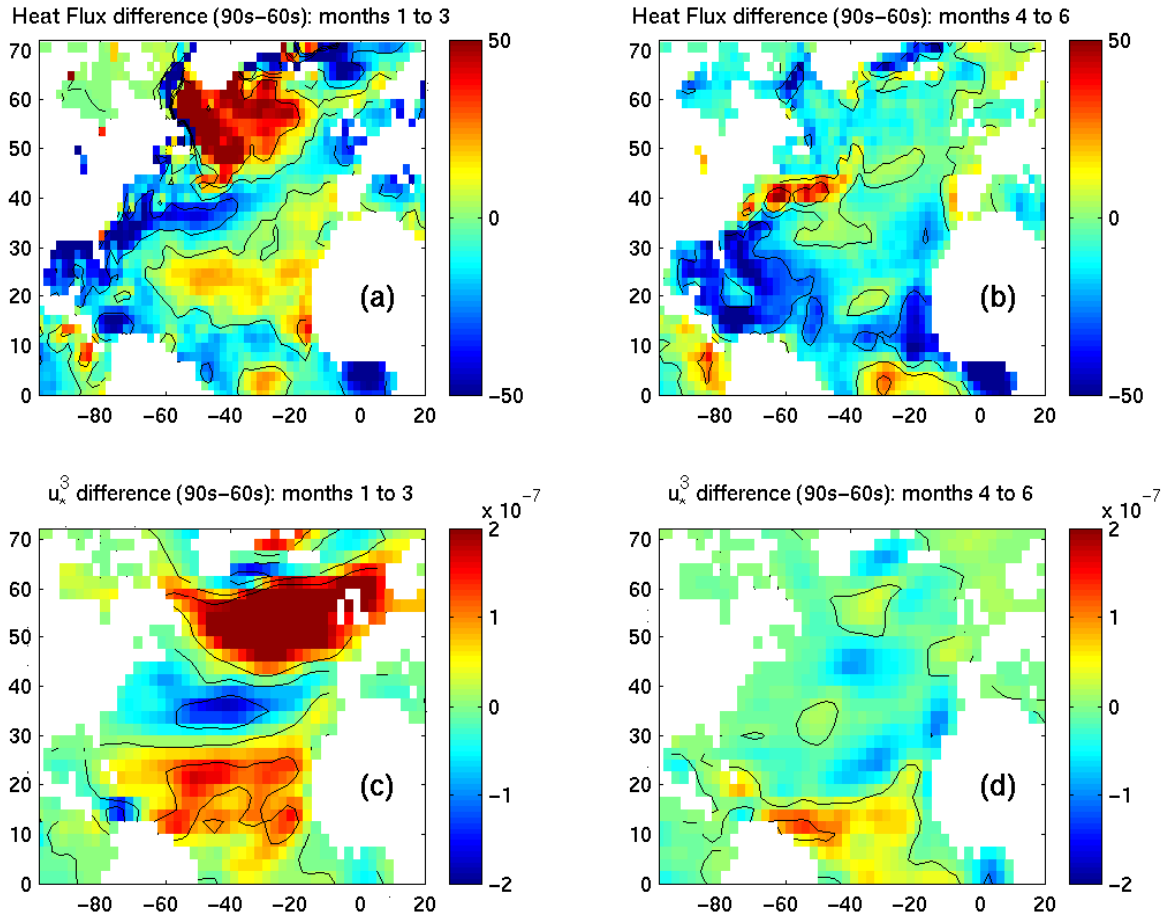

Fig. 12. Difference in the decadal climatologies of seasonal, total air-sea heat flux (a, b), and the cube of the friction velocity (u_*^3) (c, d), between the 1990s and 1960s. The left panel illustrates the difference pattern for winter months (Jan-Mar), and the right panel, the spring months (Apr-Jun). The 10 year seasonal climatologies were determined from NCEP reanalysis data for the decades of the 1990s and 1960s, and differenced for the winter and spring seasons. The total air-sea flux includes contributions from sensible and latent, and long- and short-wave radiative fluxes.

(Cayan, 1992) with stronger sea-to-air heat fluxes in the subpolar region in the 1990's (high NAO phase). However, clear patterns do not emerge in the late spring and summer months (right panel of Fig. 12). Decadal changes in u_*^3 also exhibit clear regional patterns in the winter, but not in the spring-summer.

We speculate, based on our analysis of the relatively short SeaWiFS, BATS and OWS "I" records, that the North Atlantic spring bloom may have shown a clear and predictable change in the subtropics between the 1960's and 1990's. In the subtropical regime, the surface bloom occurs in the winter, due to the enhanced nutrient supply. At this time of year, the meteorological fields which drive boundary layer mixing in the ocean exhibit clear regional patterns of inter-decadal change, typically associated with the NAO. In the western subtropics, reduced winter (January-March) heat loss from the ocean and

friction velocity in the 1990's (relative to the 1960's) suggests shallower mixed layers, reduced nutrient supply and a weaker bloom. The converse is true for the eastern subtropics. Thus we speculate that the bloom in the 1960's would have been stronger than that of the 1990's in the western subtropical gyre, but weaker in the eastern subtropical gyre.

The inference is not so clear for the subpolar gyre. The subpolar nutrient supply is strongly linked to winter (January-March) mixing anomalies, which should be enhanced in the 1990's relative to the 1960's according to the heat flux anomalies. However, the subpolar regime bloom occurs in the late spring and summer, induced by restratification. At this time of year (April-June) the meteorological forcing shows no clear inter-decadal pattern, leading to no clear inference about changes in the restratification and bloom intensity. Indeed, our analysis of the short time-series of remote observations suggests that local, interannual changes in the subpolar bloom are not simply related to local meteorology. We believe this is, in part, due to the significant role of baroclinic eddies in the restratification process and the onset of the bloom or ecological complexity. We further speculate, then, that the subpolar region is unlikely to have shown a clear change in the bloom between the 1990's and 1960's since the meteorological conditions during the critical restratification period do not show a significant pattern of change.

These speculations, based on our analysis of the recent data sets, will be examined within the framework of a multi-decadal, time-varying, physical-biological model of the North Atlantic and using available historical data. The true test and understanding of such projections will emerge, however, through continued high quality observations, both from *in situ* time-series and remote platforms, over the coming decades.

Acknowledgements

We thank Watson Gregg for useful discussions and for providing the PAR climatology used in this study. Comments and suggestions from three anonymous reviewers have helped clarify our understanding and improved this paper. SeaWiFS data was provided by the Earth Observing System Data and Information System (EOSDIS), Distributed Active Archive Center at Goddard Space Flight Center. Meteorological data products were provided by NCEP, and we thank Charmaine King for assistance in processing them. We are grateful for the data from the Bermuda Atlantic Time-series Station (BATS) and Hydrostation S programs, funded by grants from the National Science Foundation to the Bermuda Biological Station for Research, Inc., and for data from Ocean Weather Station "India" kindly provided by the PRIME program. This study was funded by NASA; grant number NCC5-244.

References

Aebischer, N.J., J.C. Coulson and J.M. Colebrook, Parallel long-term trends across four marine trophic levels and weather, *Nature* **347**, (1990) 753–755.

Cayan, D.R., Latent and sensible heat flux anomalies over the northern oceans: The connection to monthly atmospheric circulation, *J. Climate* **5**, (1992) 354–369.

Cushing, D.H., The seasonal variation in oceanic production as a problem of population dynamics. *J. du conseil int. pour l'explor. de la mer* **24** (1959) 455 – 464.

Dickson, R., J. Lazier, J. Meinke, P. Rhines and J. Swift, Long term, coordinated changes in the convective activity of the North Atlantic. *Prog. Oceanog.* **38**, 241 – 295.

Dugdale, R.C., Modeling. In *The Sea*, Vol 6, E.D. Goldberg *et al.* (Eds.), J.Wiley, New York, (1977) 789–806.

Dutkiewicz, S., M. Follows, J. Marshall and W.W. Gregg, Interannual Variability of Phytoplankton Abundances in the North Atlantic. *Deep-Sea Res.* (2001) in press.

Frommentin, J.M. and B. Planque, *North Atlantic oscillation and year-to-year plankton fluctuations.* http://www.npm.ac.uk/sahfos/staff/nao.html, (1998)

Fuentes, M., S.C. Doney, D.M. Glover and S.J. McCue, Spatial structure of the SeaWiFS ocean color data for the North Atlantic Ocean. In: *Studies in Atmospheric Sciences*. L.M. Berliner, D. Nychka and T. Hoar (Eds.), (Springer, 2000) 153–171.

Hitchcock, G.L. and T.J. Smayda, The importance of light in the initiation of the 1972–1973 winter-spring diatom bloom in Narragansett Bay. *Limnol. and Oceangr.* **22** (1977) 126–131.

Hurrell, J.W., Decadel trends in the North Atlantic Oscillation: Regional temperature and precipitation. *Science* **269** (1995) 676–679.

Jones, H. and J. Marshall, Restratification after deep convection. *J. Phys. Oceanogr.* **27** (1997) 2,276–2287.

Kalney, E., M. Kanamitsu, R. Kistler, W. Collins, D. Deaven, L. Gandin, M.M. Chelliah, W. Ebisuzaki, W. Higgins, J. Janowiak, K.C. Mo, C. Ropelewski, J. Wang, R. Jenne and D. Joseph, The NCEP/NCAR 40-year reanalysis project. *Bulletin of the American Met. Soc.* **77** (1996) 437–472.

Kennelly, M.A., J.A. Yoder, B.M. Uz and S. Doney, Satellite studies of winter-spring phytoplankton chlorophyll transitions in the North Atlantic. *EOS*, bf Suppl. 80, (2000) OS64.

Kraus, E.B., Merits and defects of different approaches to mixed layer modelling. *Small scale turbulence and mixing in the ocean*, J.C.J. Nihoul and B.M. Jamart (Eds.), (Elsevier, 1988) 37–50.

Kraus, E.B. and J.S. Turner, A one-dimensional model of the seasonal thermo-

cline. Part II: The general theory and its consequences. *Tellus* **19** (1967) 98–106.

Kraus, E.B., R. Bleck and H.P. Hanson, The inclusion of a surface mixed layer in a large-scale circulation model. *Small scale turbulence and mixing in the ocean*, J.C.J. Nihoul and B.M. Jamart (Eds.), (Elsevier, 1988) 51 – 62.

Levitus S. and T. Boyer, *World Ocean Atlas 1994 Volume 4: Temperature*, NOAA Atlas NESDIS 4, (U.S. Department of Commerce, Washington, D.C. 1994).

Lévy, M., L. Mémery and G. Madec, The onset of a bloom after deep winter convection in the North Western Mediterranean sea: mesoscale process study with a primitive equation model. *J. Marine Sys.* bf 16 (1998) 7–21.

McGillicuddy, D.J. and A.R. Robinson, Eddy induced nutrient supply and new production in the Sargasso Sea. *Deep-Sea Res.* **44** (1997) 1,427–1,449.

McGillicuddy, D.J., A.R. Robinson, D.A. Siegal, H.W. Jannasch, R. Johnson, T.D. Dickey, J. McNeil, A.F. Michaels and A.H. Knap, Influence of mesoscale eddies on new production in the Sargasso Sea. *Nature* **394** (1998) 263–266.

Menzel, D.W. and J.H. Ryther, Annual variations in primary production of the Sargasso Sea off Bermuda. *Deep-Sea Res.* **7** (1961) 282–288.

Michaels, A.F., A.H. Knap, R.L. Dow, K. Gundersen, R.J. Johnson, J. Sorennsen, A. Close, G.A. Knauer, S.E. Lohrenz, V.A. Asper, M. Tuel and R. Bidigare, 1994. Seasonal patterns of ocean biogeochemistry at the U.S. JGOFS Bermuda Atlantic Time-series Study site. *Deep-Sea Res.* **41** (1994) 1,013–1,038.

Niiler, P.P. and E.B. Kraus, One-dimensional models of the upper ocean. *Modelling and prediction of the upper layers of the ocean*, E.B. Kraus (Ed), (Pergamon, 1977) 143–172.

Reid, P.C., M. Edwards, H.G. Hunt and A.J. Warner, Phytoplankton change in the North Atlantic. *Nature* **391** (1998) 546–548.

Riley, G.A., A theoretical analysis of the zooplankton population of Georges Bank. *J. Marine Res.* **6** (1947) 104–113.

Stramska, M, T.D. Dickey, A. Plueddemann, R. Weller, C. Langdon and J. Marra, Bio-optical variability associated with phytoplankton dynamics in the North Atlantic ocean during spring and summer of 1991. *J. Geophys. Res.* **100** (1995) 6,621–6,632.

Sverdrup, H.U., On conditions of the vernal blooming of phytoplankton. *J. du conseil int. pour l'explor. de la mer* **18** (1953) 287–295.

Taylor, A.H. and J.A. Stephens, Latitudinal displacement of the Gulf Stream (1966 to 1977) and their relation to changes in temperature and zooplankton abundances in the NE Atlantic. *Oceanology Acta* **3** (1980) 145–149.

Townsend, D.W., L.M. Cammen, P.M. Holligan, D.E. Campbell and N.R. Pettigrew, Causes and consequences of variability in the timing of the spring phytoplankton blooms. *Deep-Sea Res.* **5** (1994) 747–765.

Uz, B.M., J.A. Yoder and V. Osychny, Pumping of nutrients to ocean surface

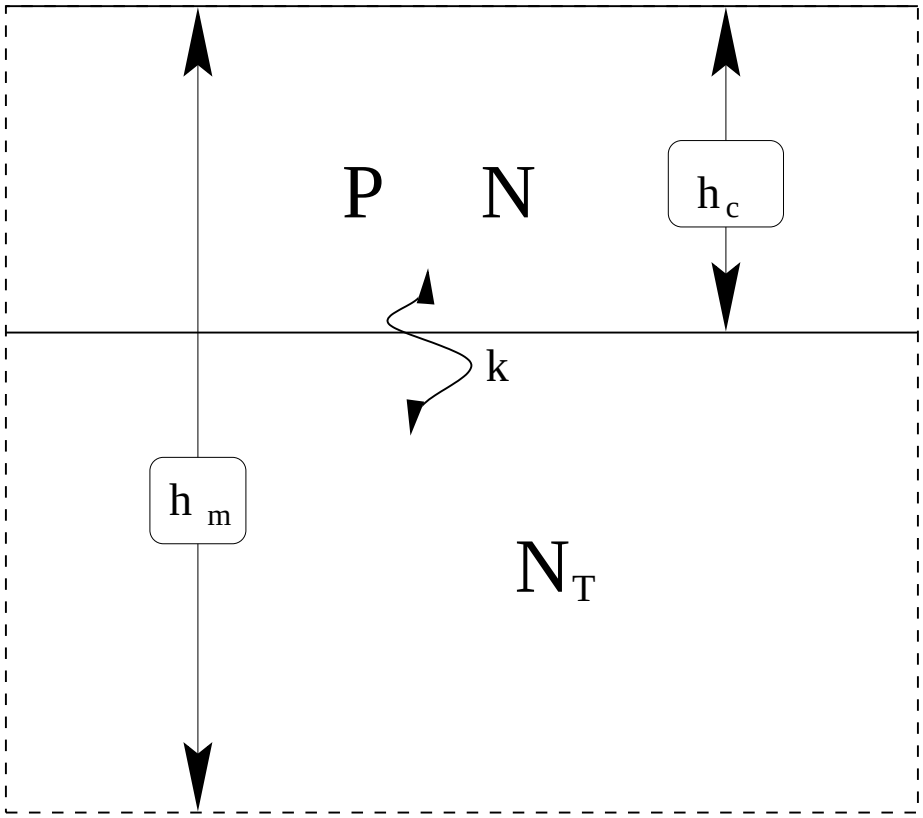

Fig. A.1. Schematic of two layer system used in Eqs. A.1, representing the end of winter mixed layer (seasonal boundary layer), h_m in which is embedded the critical layer h_c. P and N denote upper layer phytoplankton and nutrient concentrations respectively, and N_T is the nutrient concentration in the remainder of the seasonal boundary layer. The mixing coefficient, κ, represents the vertical stirring of the boundary layer caused by meteorological forcing on the surface of the ocean.

waters be the action of propagating planetary waves. *Nature* **409** (2001) 597–600.

Williams, R. and G.A. Robinson, Primary production at Ocean Weather Station India (59^o 00'N, 19^o 00'W) in the North Atlantic. *Bull. Marine Ecol.* **8** (1973) 115–121.

Williams, R.G. and M.J. Follows, Estimating new production over the North Atlantic due to the climatological Ekman supply of nutrients. *Deep-Sea Res.* **45** (1998) 461–489.

Yoder, J.A., C.R. McClain, G.C. Feldman and W.E. Esaias, Annual cycles of phytoplankton chlorophyll concentrations in the global ocean: A satellite view. *Global Biogeochem. Cycles* **7** (1993) 181–193.

A Appendix: A Two-layer Light and Nutrient Limited Bio-Physical Model

We provide a brief overview of the simple model developed in Dutkiewicz et al.(2001). The highly idealized, two layer physical-ecological model, depicted schematically in Figure A.1, is a tool for exploring the interplay between the supply of nutrients by convection and the availability of light during the spring bloom. Two layers represent the end of winter mixed layer, or seasonal boundary layer (h_m): the depth to which intermittent mixing might occur. Embedded within this is the critical layer, h_c, defined as the depth above which, in the absence of nutrient limitation, there would be a net growth in phytoplankton. In this critical layer there is a phytoplankton abundance, P, and macro-nutrient concentration, N. The remainder of the mixed layer ($h_m - h_c$) is disphotic. We describe the system as follows:

$$\begin{aligned}
\frac{dN}{dt} &= -\mu\frac{N}{(N+N_o)}P + \kappa(1-\frac{h_c}{h_m})(N_T - N) \\
\frac{dP}{dt} &= +\mu\frac{N}{(N+N_o)}P - \beta P - \kappa(1-\frac{h_c}{h_m})P \\
N_T &= constant \\
P_T &= 0.
\end{aligned} \tag{A.1}$$

The growth of plankton is described by a Michaelis-Menton parameterization (Dugdale, 1977), with half-saturation nutrient concentration of N_o and a maximum growth rate of μ. Losses due to metabolism and grazing are represented simply as βP (where β is the loss rate), and are assumed not to be re-available for biological production during the bloom period. Zooplankton and dissolved organic matter are not explicitly represented. Growth rate μ is held constant for the mean bloom period. The lower layer nutrient concentration (N_T) is fixed assuming a relatively large reservoir, and phytoplankton concentration (P_T) is zero, assuming that mortality and grazing strongly dominate the disphotic zone. Vertically and temporally averaged, mean bloom-time mixing within the seasonal boundary layer is represented by the rate constant κ, and its influence is scaled by the relative thickness of the layers ($1 - h_c/h_m$). The mixing rate, κ, may be though of as reflecting the storminess during the bloom period, or the resistance to restratification. When $\kappa = 0$ the water column is restratified, large κ represents a stormy period with more vigorous than average mixing.

Our focus is on the influence of variability of mixing during the bloom period which is, in turn, induced by interannual and spatial variability in air-sea interactions. We investigate the sensitivity of phytoplankton to the physical parameters κ and h_c/h_m by integrating the Eqns.(A.1) over the bloom period

in appropriate ranges of h_c/h_m and κ. We initialize the integration with reasonable values of N and P for end of winter conditions and plausible choices of μ, N_o, N_T and β.

Figure 2 shows the bloom period (two month) average phytoplankton concentrations normalized by N_T for time-dependent integrations of the system. The results are qualitatively robust for a range of reasonable initial conditions and parameters. Anomalously increased mixing may lead to increased or decreased phytoplankton concentrations, and this behavior is governed by the ratio of the critical depth to the mixed layer depth and vigor of the mixing. We depict results (Fig. 2) for two regimes of h_c/h_m, (subpolar, $h_c/h_m < 0,4$ and subtropical, $0.6 < h_c/h_m < 1$), and highlight solutions in parameter space appropriate for those broad regimes.

In the subtropical regime, where h_c/h_m is close to 1, an increase in mixing enhances the phytoplankton concentration by supplying increased nutrients to the upper layer. In the subpolar regime, however, springtime mixing may still be vigorous (Stramska et al., 1995) producing sufficient turbulent mixing within the boundary layer such that $(1 - h_c/h_m)\kappa$ is large. According to this simple model, and as illustrated by the area between the curves in Figure 2 at higher mixing rates, phytoplankton concentrations diminish with enhanced mixing. With very high mixing rates though, the model suggests that phytoplankton concentrations become quite low and less sensitive to further enhancement of mixing.

FIGURE CAPTIONS.

Figure 1. Upper panel: Two year mean (1998 and 1999) surface chlorophyll concentration (mg/m^3) from SeaWiFS (Level 3, version 3) estimates. Lower panel: Relative difference (1999-1998) presented as a percentage of the mean. Contours are overlaid for -50%,-25%, 0%, 25% and 50% of the difference field.

Figure 2. Bloom period mean surface phytoplankton concentrations, normalized by winter mixed layer nutrient concentration (P/N_T), as a function of the springtime vertical mixing rate within the seasonal boundary layer, κ from the idealized, two-layer, bio-physical model (see Appendix and Dutkiewicz et al., 2001). Solid lines indicate the solutions for the values of h_c/h_m bounding the regimes of interest. Shaded areas indicate all possible solutions within those regimes. (a) low h_c/h_m ratios ("subpolar" regime) and (b) high h_c/h_m ("subtropical"). The figure illustrates the predicted qualitative difference in chlorophyll in response to regional or interannual changes in spring time mixing. The broad, shaded swaths indicated the predicted spread of data for these broad classes of h_c/h_m. The values for μ, N_o and β are 1.5 d^{-1}, 0.1 μM and 0.5 d^{-1}, respectively for these experiments.

Figure 3. Bloom-period (1998), SeaWiFS surface chlorophyll (mg/m^3) averaged in $5^o \times 5^o$ bins. The months defined as the bloom-period (see text) are indicated for each latitude band.

Figure 4. Climatological: (a) h_c, spring critical layer depth (m); (b) h_m, end of winter mixed layer depth (m); (c) h_c/h_m.

Figure 5. Total air-sea heat flux for the 1998 bloom period (W/m^2, positive out of the ocean). Data from NCEP re-analysis, are averaged for the bloom period as defined in Figure 3. The total heat flux includes contributions from sensible and latent heat exchanges, along with long and short wave radiative fluxes. The subtropical gyre is losing heat and unstable during its bloom, while the subpolar gyre is gaining heat and restratifying.

Figure 6. (a) Bermuda Atlantic Time-Series (BATS) upper 10m chlorophyll concentration (mg/m^3) from 1990 to 1996; (b) Scatter plots of bloom-period, upper 10m chlorophyll against total heat air-sea heat flux, H_o; friction velocity cubed and TKE generation (Eq. 1). All data are averaged over January and February for each year (1990 to 1996). Mixed layer depths for Eq. 1 are determined from *in situ* density measurements.

Figure 7. (a) OWS "India" upper 10m chlorophyll concentration (mg/m^3). (b) Scatter plots of OWS "I" upper 10m chlorophyll against total air-sea heat flux, H_o; friction velocity cubed; and TKE generation (Eq. 1). All data are averaged over May and June for each year (1971 to 1975). Mixed layer depths for Eq. 1 are determined from *in situ* temperature measurements. Hydrography and

mixed layer depth are unavailable for 1973, precluding an estimate of TKE generation for that bloom.

Figure 8. Bloom Period (1998) SeaWiFS chlorophyll (mg/m^3) plotted against NCEP total heat flux (W/m^2) and friction velocity, u_*^3 ($\times 10^{-6}$ m^3/s^3) derived from NCEP wind stress data. Each data point indicates the 1998 "bloom" average for one five degree bin (Fig. 3). We separate the results into subpolar and subtropical regimes according to broad classes of the local value of h_c/h_m (ranges indicated above figure). Left column shows results for the small h_c/h_m, subpolar regime; the right column shows results for the high h_c/h_m, subtropical regime. The shaded regions indicate one standard deviation either side of a linear least squares fit (see text for discussion).

Figure 9. Regional variability in the spring bloom. Bloom Period (1998) SeaWiFS chlorophyll (mg/m^3), plotted against TKE generation (derived using equation (1) and monthly, climatological mixed layer depth h). Data grouped by broad h_c/h_m classes reflecting the subpolar (low h_c/h_m) and subtropical (high h_c/h_m) regimes. The h_c/h_m classes are defined above the figure. Generation of TKE is assumed to be proportional to the rate of vertical mixing within the seasonal boundary layer. Compare the trends and spread in the data with the idealized model results in Figure 2.

Figure 10. Interannual and regional variability in the bloom. SeaWiFS level 3 chlorophyll (mg/m^3) for each of the three blooms observed to date (1998 o, 1999 x, 2000, $*$) plotted against (upper panel) heat flux (W/m^2); (middle panel) friction velocity, u_*^3 ($\times 10^{-5}$ m^3/s^3); and (lower panel) generation of TKE ($\times 10^{-5}$ m^3/s^3), derived using (1). Low (subpolar) and high (subtropical) h_c/h_m regimes are shown. Data are averaged over the bloom period and for the five-degree bins depicted in Figure 3. Compare the trends and spread of data in the lower panels to the idealized model results in Figure 2.

Figure 11. Interannual trajectories. Annual bloom data points for each of the three observed blooms (1998, 1999, 2000) in each five-degree bin are shown. Lines join each set of three bloom data points from the same geographic bin, starting at the data point with the lowest generation of TKE and proceeding with increasing TKE generation. The left panel shows the subpolar regime, the right panel the subtropical. The subtropical regime shows clear and consistent interannual trends with stronger mixing leading to a stronger bloom. Interannual changes are of the same order as regional variations within the subtropics. The subpolar regime shows no clear interannual trends, and variability is dominated by regional changes.

Figure 12. Difference in the decadal climatologies of seasonal, total air-sea heat flux (a, b), and the cube of the friction velocity (u_*^3) (c, d), between the 1990s and 1960s. The left panel illustrates the difference pattern for winter

months (Jan-Mar), and the right panel, the spring months (Apr-Jun). The 10 year seasonal climatologies were determined from NCEP reanalysis data for the decades of the 1990s and 1960s, and differenced for the winter and spring seasons. The total air-sea flux includes contributions from sensible and latent, and long- and short-wave radiative fluxes.